

Improved performance of CdTe thin-film solar cell through key parameters

Loumafak Hafaifa^{1,2} , Mostefa Maache^{1,3,*} ,
Mohamed Wahid Bouabdelli⁴ 

¹Department of Physics, Faculty of Exact Sciences and Computer Science, Ziane Achour University, Djelfa, Algeria.

²Physico Chemistry of Materials and Environment Laboratory, Ziane Achour University of Djelfa, Djelfa, Algeria.

³Physical Laboratory of Thin Films and Applications, Mohamed Khider University, Biskra, Algeria.

⁴Faculty of Science and Technology, Djelfa University, Djelfa, Algeria.

*Corresponding author: m.maache@univ-djelfa.dz

Original Research

Abstract:

Received:
24 November 2023
Revised:
5 February 2024
Accepted:
20 March 2024
Published online:
25 May 2024

© The Author(s) 2024

We investigated CdTe thin-film solar cell configuration using Silvaco Atlas. We simulated a fundamental CdTe cell at an ambient temperature of 298 K. Subsequently, we compared our simulation results to both theoretical and experimental data. The outputs demonstrated a compelling concurrence with the performance of the experimental CdTe solar cell, renowned for its record-breaking efficiency, thereby validating our model. To surpass the current efficiency record of 22.4% for the CdTe cell, we undertook a rigorous optimization process, focusing on two important parameters: the thicknesses of the different layers and the doping densities. Following optimization, the optimal parameters determined were as follows: 20 nm -10^{19} cm⁻³ for the ZnO and CdS layers, and 3000 nm -5×10^{14} cm⁻³ for the CdTe layer. These optimized parameters resulted in a substantial enhancement, increasing the efficiency from 22.15% to 27.8%. The majority of prior research studies have assessed CdTe solar cells at standard room temperature. However, operating temperatures in real-world applications can vary significantly. We expanded our research to include temperature optimization and its impact on CdTe cell performance. Our findings revealed that performance significantly improves with reduced temperature. At a temperature of 250 K, the CdTe cell achieved an efficiency of 32.36%.

Keywords: Solar cell; CdTe thin films; Thicknesses; Doping density; Efficiency; Silvaco Atlas

1. Introduction

In response to the escalating global energy demand and the damaging environmental consequences of conventional energy sources, most notably fossil fuels, renewable energy solutions are pivotal. Solar cells have presently emerged as an indispensable and sustainable source of clean energy [1, 2]. Despite crystalline silicon forming the basis of over 80% of commercial photovoltaic (PV) modules, they exhibit limitations such as substantial material consumption and reduced cost-effectiveness [3]. Thin-film PV technologies have significantly mitigated active material consumption in solar cells, consequently enhancing cost-effectiveness. Additionally, these technologies have achieved higher efficiencies compared to conventional silicon cells [4]. Conse-

quently, as such, thin-film cells have become the preferred alternative in contemporary solar cell development initiatives, given their notable advantages over their bulky and more expensive silicon counterparts.

The primary thin-film technologies deployed in photovoltaic systems encompass CIGS, a-Si, and CdTe as absorber layers, all of which have currently reached the commercialization stage [3]. Among these technologies, CdTe photovoltaic stands out as the most cost-effective option [3, 5]. CdTe technology not only offers superior cost-efficiency but also commands a significant market share in comparison to a-Si and CIGS technologies [2, 3]. The efficiency of CdTe surpasses that of a-Si and closely approaches that of CIGS [4]. Furthermore, CdTe cells present an array of ad-

vantages, including reliability [5], flexibility [6], long-term stability [7, 8], simplicity, and cost-effectiveness [8, 9]. As an absorber material, CdTe emerges as a highly promising choice, characterized by its straightforward binary compound structure featuring wurtzite and zinc blende structures [7]. Notably, CdTe exhibits a high absorption coefficient (exceeding 10^5 cm^{-1}) and boasts a direct band gap (E_g) of 1.5 eV [7, 10–13]. Experimental CdTe solar cells have consistently achieved rising conversion efficiencies in various photovoltaic research centers. Remarkably, these cells have achieved an efficiency of 16.5% at the National Renewable Energy Laboratory (NREL) [5, 8]. The present global record efficiency, at 22.4%, has been attained at First Solar Research and Development (FSRD) [4]. Additionally, numerous theoretical and simulation studies have delved into CdTe solar cells, as evidenced by literature references [14–23]. Nonetheless, the challenge of augmenting solar cell performance endures as a central endeavor in the photovoltaic field.

In this context, the primary objective of the current study is to enhance the performance of CdTe cells, surpassing the existing efficiency of 22.4%. A secondary aim is to evaluate CdTe cells under diverse temperature conditions and explore their implications for cell performance. Two pivotal parameters are optimized to enhance CdTe cell performance: cell thickness, a key factor in augmenting performance and curtailing production costs, and doping density, a critical parameter for elevating open-circuit voltage and, in turn, cell performance. While prior studies have predominantly maintained an operating temperature of 298 K for solar cells [4]. Temperature differences between areas varied significantly depending on time of day and month of the year, as well as owing to the installation of photovoltaic panels in diverse geographic regions. Therefore, it is imperative to investigate the performance of CdTe cells across a range of temperatures. To achieve this, we have investigated the influence of operating temperature on the cell's performance parameters.

In this work we have employed the Silvaco-Atlas numerical simulation program. Our methodology encompasses the initial design of a foundational CdTe solar cell, which is benchmarked against performance parameters derived from prior experimental and simulated cells. Subsequently, we have conducted an exploration of various layer thicknesses and doping densities to ascertain their optimal values. By incorporating these optimal parameters, we have devised the optimized cell, the performance of which is juxtaposed with that of the basic cell. Furthermore, we have investigated the influence of operating temperatures on the cell's performance parameters.

2. Materials and methods

2.1 Description of numerical modeling

In scientific investigation, models and simulations rooted in actual physical phenomena have become critical tools for unraveling the operational intricacies of devices and their fundamental mechanisms. Such techniques, easily accessible, economical, and with accelerated turnaround compared to experimental studies. They have the potential to reveal

pivotal insights that often escape detectability in empirical studies. Amid such potent tools, one finds Silvaco-Atlas a notable simulation platform chosen by global researchers to scrutinize and boost the performance of semiconductor devices. Silvaco-Atlas's value lies in its ability to accurately predict thermal, electrical, and optical characteristics in both traditional and cutting-edge semiconductor devices, notably complex physical structure ones such as solar cells [24].

In the framework of the current study, Silvaco Atlas assumes an integral part in the modeling and enhancement of CdTe solar cells, utilizing rudimentary semiconductor equations, which include the continuity equation and the Poisson equation that govern charge carriers, electrons and holes [24–26].

The I-V curve, often known as the current-voltage relationship, is critical for solar cell performance. Total current is computed by combining photocurrent (I_{ph}) and dark current. The relationship shows how the dark and photocurrent combine to generate total current, as expressed by the well-known Shockley equation:

$$I = I_{ph} - I_0 \left(\exp\left(\frac{qV}{akT}\right) - 1 \right) \quad (1)$$

where I is the current flowing through the solar cell, I_0 is the saturation reverse current, q is the electron charge, V is the applied voltage, a is the ideality factor, k is the Boltzmann constant, and T is the absolute temperature.

- The I_{SC} (short-circuit current) when $V = 0$:

$$I_{SC} = I_{ph} \quad (2)$$

- The V_{OC} (open circuit voltage):

$$V_{OC} = \frac{akT}{q} \ln\left(\frac{I_{ph}}{I_0}\right) \quad (3)$$

- The FF (fill factor):

$$FF = \frac{P_{max}}{V_{OC}I_{SC}} \quad (4)$$

- The η (Efficiency):

$$\eta = \frac{P_{max}}{P_{in}} = \frac{V_{OC}I_{SC}FF}{P_{in}} \quad (5)$$

P_{max} is the maximum power, and P_{in} is the incident optical power.

2.2 Structure and material characteristics of CdTe solar cell

A CdTe cell fundamentally consists of several thin-film layers meticulously organized in a sequential order. Commencing from the glass substrate, the structure features an n-doped ZnO (200 nm), dual-purpose in its roles as both a TCO (Transparent Conductive Oxide) and the anterior contact. Subservient to this is the n-doped CdS (100 nm) layer acting as the buffer layer. The subsequent layer incorporates a p-doped CdTe (1000 nm) serving as the absorber layer. Concluding this sequence is the metallic layer that functions as the rear contact as shown in Figure 1. This selected layer

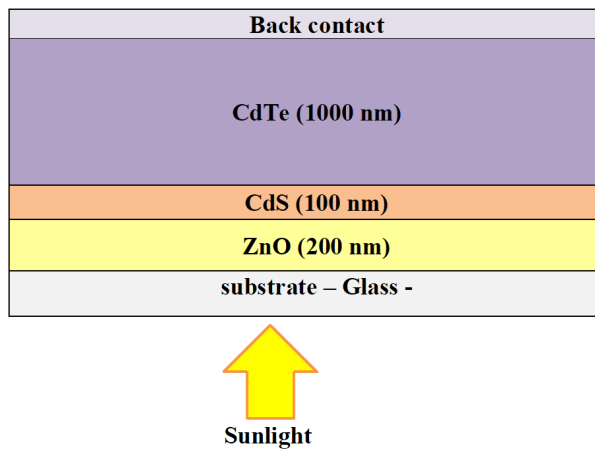


Figure 1. Structure of the fundamental CdTe cell.

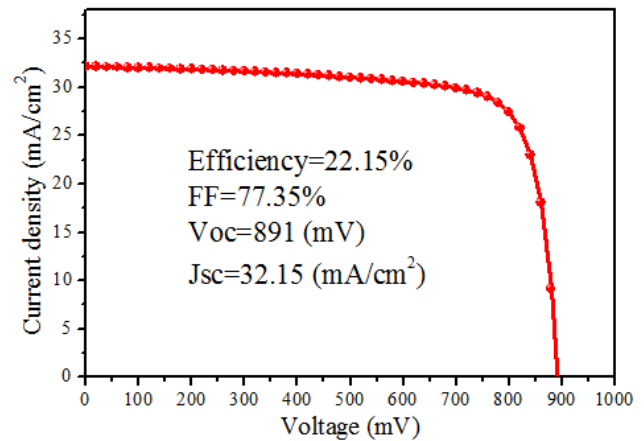


Figure 2. Current-voltage characteristics of the fundamental CdTe cell.

organization leans on insights gathered from a wide collection of studies [5–22, 27]. When utilizing Silvaco Atlas for the emulation of the CdTe cell, individual parameters are allocated to each cell constituent. This emulation operates under Standard Test Conditions (298 K, AM1.5G, and 100 mW/cm²) [4]. Pulling from empirical evidence noted in extant literature, we derive the optical parameters for the ZnO and CdS layers [28, 29]. Conversely, the optical determinants for CdTe are accessible through the Silvaco Atlas library's SOPRA database [24].

The electrical attributes for all materials employed in this simulation are sourced from various references [4, 7, 14–22, 27, 30]. For a detailed enumeration of these electrical parameters, please refer to Table 1.

3. Results and discussion

3.1 Evaluation of the fundamental CdTe cell

The simulation of the fundamental CdTe cell was carried out using the parameters specified in Table 1. The results of this simulation are demonstrated in Figure 2, which presents the J-V curve. Additionally, Table 2 provides the photovoltaic performance parameters associated with this simulation. In order to validate the accuracy of our model, we compared the performance parameters obtained from our simulation with those derived from the highest recorded efficiency cell, as well as other simulated cells. Table 2 offers a comprehensive summary of this comparative analysis, highlighting the key parameters for solar cell performance, including η ,

FF , V_{OC} , and J_{sc} .

The results presented in Table 2 demonstrate a significant agreement between the performance of our simulated cell model and the experimental results reported in [4]. Notably, our model outputs surpass those of the simulated cell presented in previous study [14]. This tough alignment provides substantial support for the validity of our model and the parameter set utilized in our simulation, establishing a reliable foundation for subsequent simulations carried out within this study.

3.2 Optimizing of CdTe cell

After identifying the CdTe cell structure, the subsequent objective is to enhance their photovoltaic parameters, such as η , FF , V_{OC} , and J_{sc} . The strategy involves the precise regulation of key parameters that significantly influence their overall efficiency. These crucial parameters primarily necessitate meticulous calibration of layer thickness and control of doping concentration. Through a comprehensive and structured examination of the impact of these parameters on efficiency, our ultimate aim is to establish an optimized cell to attain the highest possible efficiency.

3.2.1 Optimizing CdTe cell structure

The optimization process of the CdTe cell structure involved adjusting the thickness of each layer while keeping the other layers' thickness constant. The objective was to find the ideal thicknesses values that can improve the cell's perfor-

Table 1. Different material parameters used in the simulation of CdTe cell.

Parameters	p-CdTe	n-CdS	n-ZnO
Energy Bandgap, E_g (eV)	1.5	2.4	3.3
Doping density (N_A, N_D) (cm ⁻³)	$N_A = 10^{15}$	$N_D = 10^{19}$	$N_D = 10^{19}$
Relative Permittivity, ϵ_r (F cm ⁻¹)	9.4	10	9
Electron affinity, χ (eV)	4.28	4.18	4.5
Density of states at Conduction Band, N_c (cm ⁻³)	8×10^{17}	2.2×10^{18}	2.2×10^{18}
Density of states Valance Band, N_v (cm ⁻³)	1.8×10^{19}	1.8×10^{19}	1.8×10^{19}
Hole mobility μ_p (cm ² /V s)	40	25	25
Electron mobility μ_n (cm ² /V s)	320	100	100

Table 2. Performance parameters of the fundamental CdTe cell.

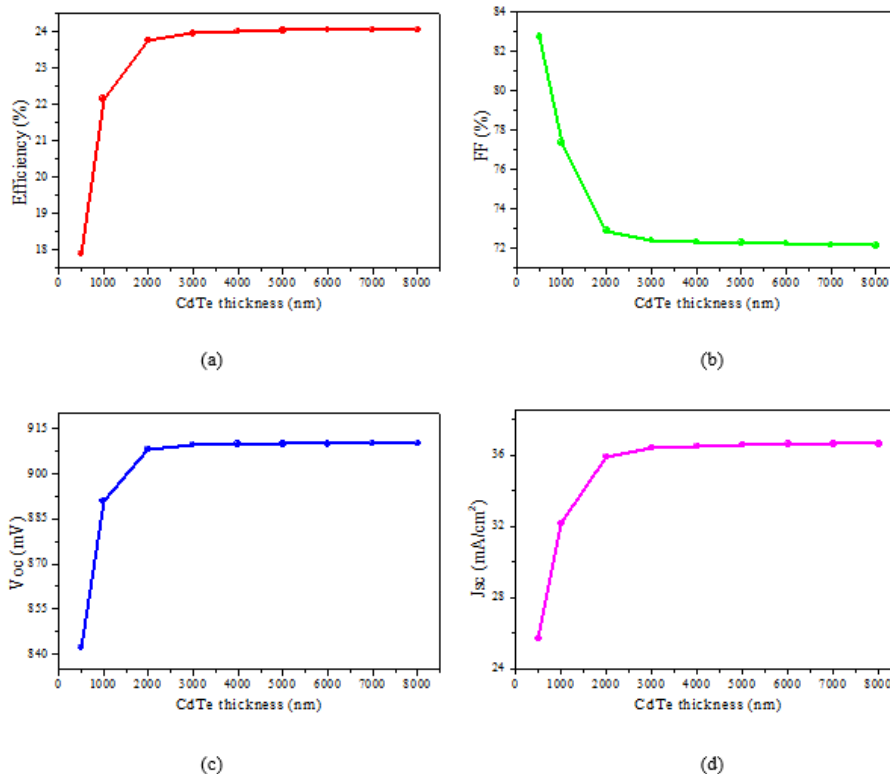
Performance parameters	Other Simulated cell [14]	The experimental cell [4]	Our simulated cell
Efficiency η (%)	22.14	22.4	22.15
FF (%)	78.89	79.3	77.35
V_{OC} (mV)	884	899.6	891
J_{sc} (mA/cm ²)	31.73	31.4	32.15

mance.

The thickness of the CdTe was varied between 500 and 8000 nm, while maintaining the thickness of the other layers: CdS at 100 nm and ZnO at 200 nm. Figure 3 illustrates the primary performance parameters, such as efficiency (η), FF , J_{sc} , and V_{OC} , as a function of the CdTe thickness. Figure 3 clearly shows that increasing the CdTe thickness has a significant impact on these performance parameters. In the range of 500 to 3000 nm, increasing the CdTe thickness results in a decrease in FF from 82.74% to 72.3%. This decrease can be attributed to increased bulk resistance and series resistance due to the thicker CdTe layer. However, within this range; J_{sc} , V_{OC} , and efficiency (η) exhibit significant increases. Specifically, the efficiency increases from 17.8% to 23.96%, accompanied by a decrease in FF . Beyond 2500 nm, these values stabilize. Consequently, the optimal CdTe layer thickness, where the efficiency peaks at 23.96%, is determined to be 3000 nm. The increase in efficiency can be attributed to the higher absorption of photons with increasing CdTe thickness, resulting in a greater number of electron-hole pairs and an increased photocurrent (I_{ph}), V_{OC} , and overall efficiency. However, further

increases in CdTe thickness surpass the diffusion length, rendering the additional light absorbed non-contributory to the photocurrent. This observation aligns with findings from a previous study [22].

In the second phase, the thickness of the CdS layer was systematically adjusted between 20 and 200 nm, while keeping the dimensions of the other layers constant: CdTe at 1000 nm and ZnO at 200 nm. Figure 4 presents a comprehensive overview of the key performance parameters as a function of the CdS thickness. It demonstrates an improvement in all performance parameters as the CdS layer thickness increases from 20 to 200 nm. Notably, there is a sharp decline in efficiency from 24% to 21%, representing a 3% decrease. This decrease can be attributed to the higher photon absorption capacity of a thicker CdS layer, a finding corroborated by similar experimental results previously reported [31], limiting the number of photogenerated carriers and thus, the photocurrent in the absorber layer. Consequently, the performance parameters dependent on photocurrent also decrease. The maximum efficiency of 24% is achieved at a CdS thickness of 20 nm, identifying it as the optimal CdS thickness that enhances cell performance while reducing

**Figure 3.** Effect of CdTe layer thickness on cell performances: (a) η , (b) FF , (c) V_{OC} , (d) J_{sc} .

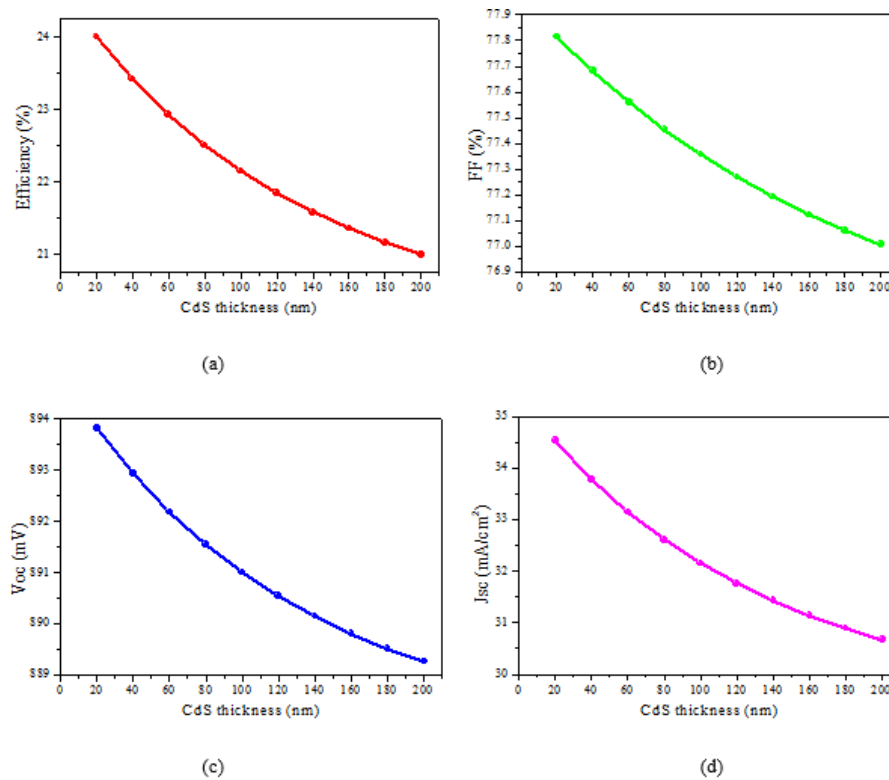


Figure 4. Effect of CdS layer thickness on cell performances: (a) η , (b) FF , (c) V_{OC} , (d) J_{sc} .

overall thickness.

In the final phase, the thickness of the ZnO (TCO) layer was varied between 20 and 260 nm, while keeping the thickness of the other layers constant CdTe at 1000 nm and CdS at 100 nm. Figure 5 provide insights into the primary performance parameters in relation to the ZnO thickness.

Figure 5 demonstrates that increasing the ZnO thickness from 20 to 260 nm leads to a modest improvement in all performance parameters. Since ZnO serves as a transparent conducting oxide, its exceptional transparency characteristics are limited. A thicker ZnO layer tends to absorb a significant number of photons that could reach the absorber layer, resulting in a reduction in photogeneration and subsequently, a decrease in the cell's performance. The maximum efficiency of 22.35% is achieved at a thickness of 20 nm for the TCO layer, identifying it as the optimal ZnO layer thickness.

3.2.2 Doping density optimization

We conducted a systematic adjustment of the doping density in different layers of the CdTe thin-film solar cell, with the specific aim of identifying the optimal values that would lead to the highest performance of the cell. In particular, we focused on varying the acceptor doping density (N_A) in the CdTe absorber layer, while keeping all other parameters constant.

The range of N_A in the CdTe absorber layer was varied from 10^{14} to 10^{18} cm^{-3} . Figure 6 presents the results of this variation, showing the primary performance parameters as a function of the N_A in the CdTe layer. Several trends become apparent, as the N_A in the CdTe layer increases from 10^{14} to 3×10^{14} cm^{-3} , there is a noticeable increase in the FF .

However, beyond 3×10^{14} cm^{-3} , the FF declines before showing a rapid linear increase. On the other hand, the J_{sc} initially experiences a slight decrease as the N_A increases from 10^{14} to 10^{15} cm^{-3} , followed by a significant linear drop. This can be attributed to the reduction in the width of the depletion region, which is a significant factor contributing to photocurrent, as the N_A rises [25].

Furthermore, it is worth noting that an increase in the N_A of CdTe from 10^{14} to 10^{18} cm^{-3} leads to a significant increase in the V_{OC} by 390 mV, from 661 to 1051 mV. This increase in V_{OC} can be attributed to the inverse relationship between the N_A and the reverse saturation current I_0 , which influences V_{OC} [32]. These variations in J_{sc} and V_{OC} also have an impact on both the FF and the overall efficiency of the solar cell.

In terms of efficiency, it rapidly increases by 5.1% as N_A increases from 10^{14} to 5×10^{14} cm^{-3} , reaching a maximum efficiency of 22.35% at this doping density. Beyond 5×10^{14} cm^{-3} , the efficiency starts to decrease.

Additionally, we investigated the effect of varying the donor doping densities (N_D) in both the CdS buffer layer and the TCO layer, while keeping other parameters constant. Our observations indicate that changing the N_D had no significant impact on the performance of the solar cell. This can be attributed to the fact that most of the depletion region and potential shift occur within the CdTe absorber layer ($N_A \ll N_D$). Therefore, we concluded that the optimal donor doping densities for CdS and ZnO should remain at their initial levels.

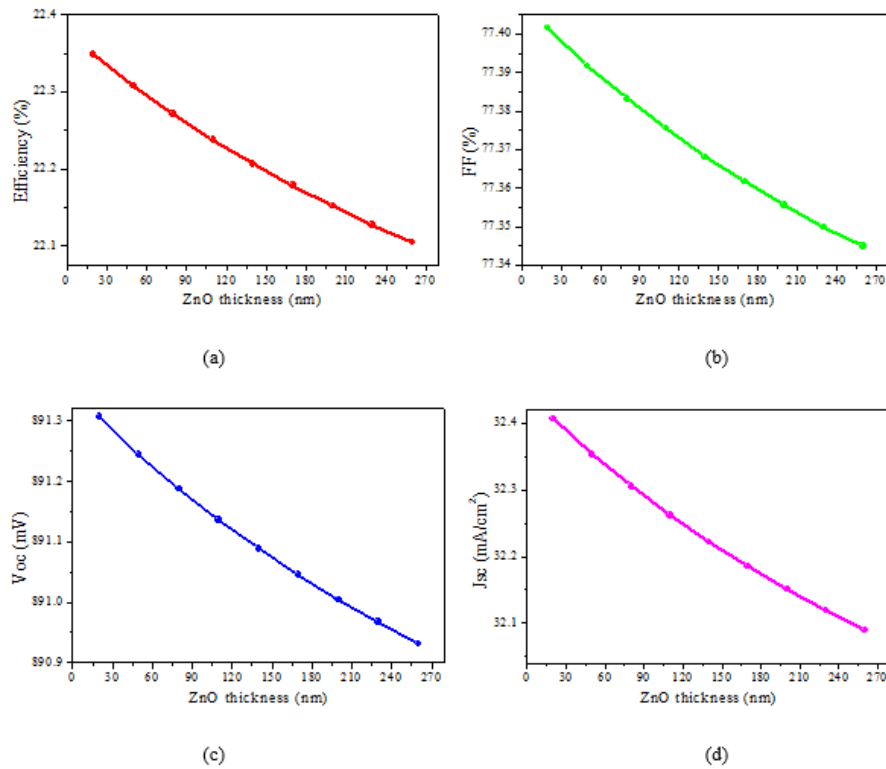


Figure 5. Effect of ZnO layer thickness on cell performances: η , (b) FF , (c) V_{OC} , (d) J_{sc} .

3.3 Improved CdTe cell

An improved CdTe cell was constructed and simulated, using specific parameters for optimizing layer thickness and doping density. These parameters included a thickness of

3000 nm and a acceptor doping density (N_A) of $5 \times 10^{14} \text{ cm}^{-3}$ for the CdTe absorber layer, a thickness of 20 nm and a donor doping densities (N_D) of 10^{19} cm^{-3} for the CdS buffer layer, and identical properties for the ZnO layer. The

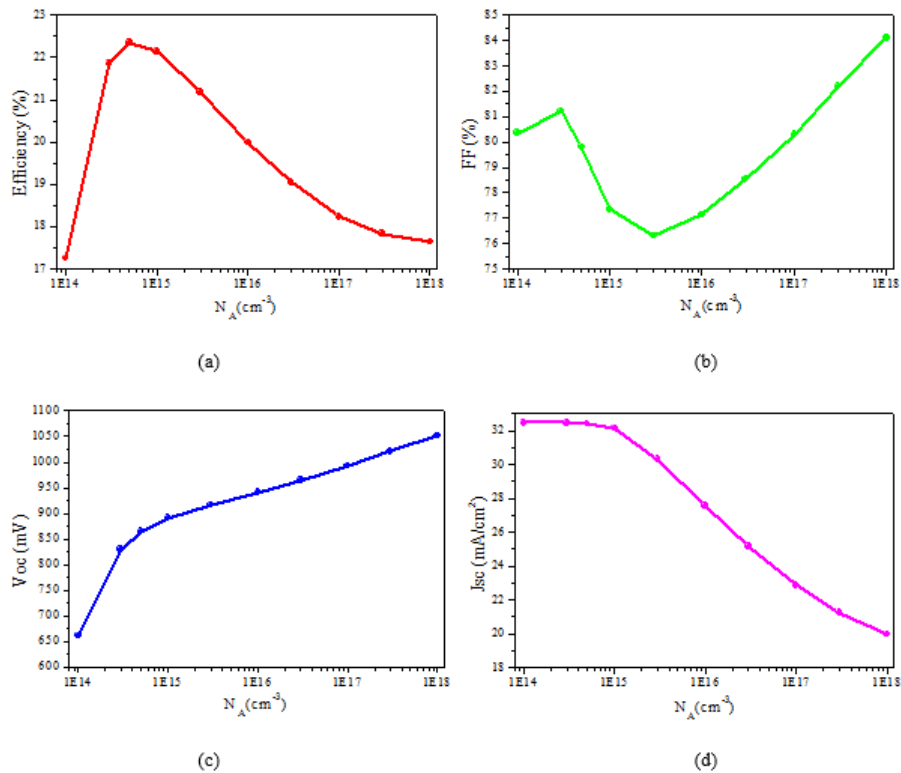


Figure 6. Effect of acceptor density on CdTe cell performances: η , (b) FF , (c) V_{OC} , (d) J_{sc} .

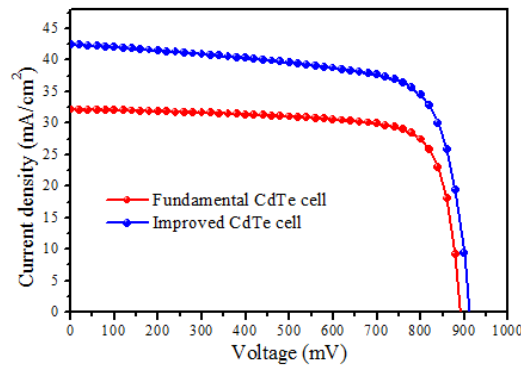


Figure 7. Current-voltage characteristics of the improved cell and the fundamental cell.

$J - V$ characteristics for both the improved and reference (fundamental cell) cells are presented in Figure 7. A detailed analysis of the performance for the improved cell is summarized in Table 3. This table facilitates an immediate and convenient comparison with the performance metrics of the fundamental cell.

Upon examination of the data presented in Table 3 and Figure 7, it becomes apparent that the optimized solar cell exhibits notable enhancements in various performance parameters. Specifically, there is a substantial increase of 20.36 mV in open-circuit voltage (V_{OC}), a gain of 10.33 mA/cm² in short-circuit current (J_{sc}), resulting in a 5.65% improvement in overall efficiency. Conversely, there is a 5.53% reduction in the fill factor (FF).

3.4 Operating temperature optimization

Our investigation into the effects of operating temperature on CdTe solar cells, aiming to define the ideal temperature, involved testing our recently optimized cell over a temperature interval of 250 to 400 K. The test outcomes are delineated in Figure 8, outlining the relationship between the performance parameters and operating temperature. This phenomenon has been extensively investigated in the literature. For instance, Asaduzzaman et al. conducted a study on a CdTe-based thin-film solar cell, revealing their sensitivity to temperature variations [33].

Insights gathered from Figure 8 highlight a significant and positive correlation between lower temperature levels and cell performance parameters. A steady linear enhancement in efficiency, V_{OC} , and FF is noted as the temperature is dropped from 400 to 250 K. Concurrent to this, J_{sc} depicts

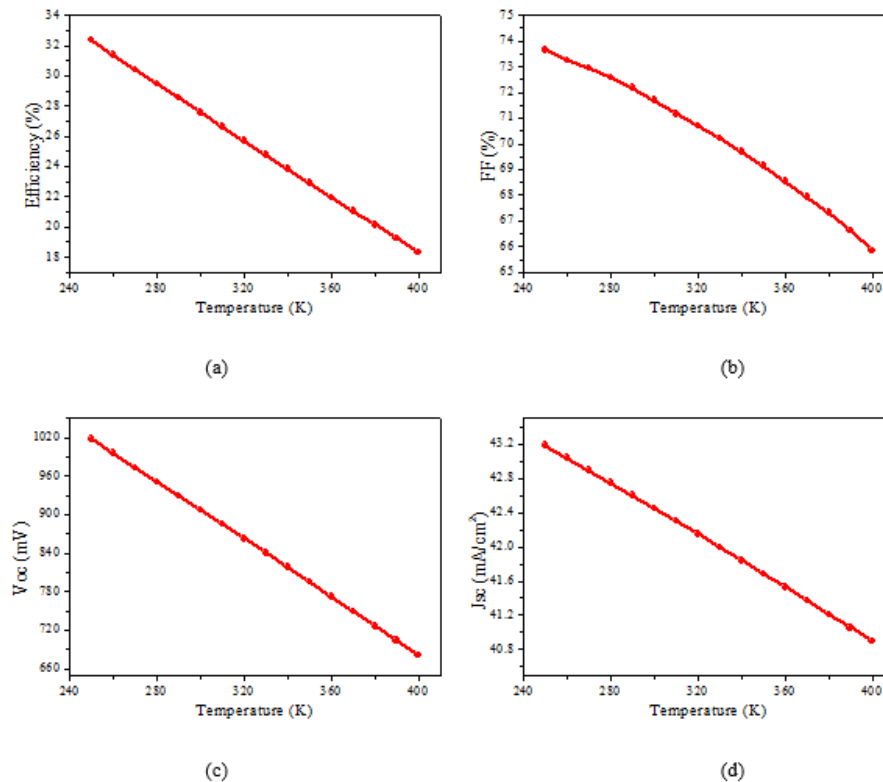


Figure 8. CdTe cell performances versus temperature: (a) η , (b) FF , (c) V_{OC} , (d) J_{sc} .

Table 3. Performance parameters of the fundamental and optimized CdTe Cell.

Performance parameters	Improved cell	Fundamental cell
Efficiency η (%)	27.8	22.15
FF (%)	71.82	77.35
V_{OC} (mV)	911.36	891
J_{sc} (mA/cm ²)	42.48	32.15

a boost by 2.29 mA/cm². It is to be noted that the augmentation in performance parameters is largely due to the significant rise in V_{OC} , resulting from its temperature-dependent nature. The subsequent enhancements in the remaining performance parameters are related to their shared dependence on V_{OC} .

Supplementing this, Figure 8 illustrates the increase in V_{OC} , from 681.3 to 1017.8 mV, as a result of the temperature drop from 400 to 250 K, which accounts for an approximate increment of 2 mV/K. Simultaneously, there is a considerable surge in efficiency, scaling from 18.34% to 32.36%. The efficiency spectrum reveals a growth rate of about 0.1%/K, clarifying that a decrease in temperature by 10 degrees can lead to a significant 1% climb in efficiency. The peak of efficiency is attained at 250 K, registering at 32.36%, which signifies an impressive rise of 4.56% in comparison with the standard room temperature performance at 298 K. Consequently, we establish 250 K as the ideal operating temperature.

In essence, a reduction in operating temperature considerably amplifies cell efficiency. This emphasizes the importance of maintaining lower operational temperatures, whenever practicable. The realization of reduced cell temperatures can be achieved through careful placement in cooler settings or by applying a variety of photovoltaic cooling measures. Several photovoltaic cooling methods, such as water-cooling and forced air-cooling, have been adopted to lower the operational temperature of solar cells and panels [34, 35]. Among these, the use of phase change materials (PCMs) in a notable conductive cooling approach shows promise. Recent studies indicate that the application of PCMs can contribute to a reduction in PV panel temperature by 35.6 K [36]. This correspondingly elevates the efficiency of the CdTe cell by 3.56%.

4. Conclusion

The conducted simulation and optimization process on the CdTe thin-film solar cell have yielded critical understanding towards the enhancement of its performance and reaching superior efficiency. The derived results affirm that tuning the layer thicknesses and optimizing the doping densities can considerably affect the cell's efficiency. Insights gained from the optimization process reveal the CdTe absorber layer's efficiency apex at a thickness of 3000 nm. Similarly, both the CdS buffer layer and the ZnO layer demonstrate optimal performance at a thickness of 20 nm. The respective doping densities for the CdTe, CdS, and ZnO layers were found to be $5 \times 10^{14} \text{ cm}^{-3}$, 10^{19} cm^{-3} , and 10^{19} cm^{-3} . Through the application of these optimal parameters, a high efficiency of 27.8% was achieved with the

CdTe solar cell. Additionally, lowering the cell's operating temperature contributed to a substantial improvement in its efficiency. Remarkably, the cell's efficiency peaked at 32.36% by maintaining an optimal temperature of 250 K, outperforming the record efficiency by 10.26%. Consequently, these results suggest that significant efficiency enhancement can be achieved by the reduction of the cell's temperature. Therefore, strategies to achieve lower cell temperature might involve placement in cooler regions or the application of specialized photovoltaic cell cooling techniques. These insights offer valuable direction for those aiming to construct high-efficiency CdTe solar cells and potentially set unprecedented benchmarks in solar cell efficiency.

Authors Contributions

Loumafak Hafaifa: Conception, Setup design, Data analysis, Draft writing; Mostefa Maache: Conception, Setup design, Data analysis, Finalizing the paper; Mohamed Wahid Bouabdelli: Conception, Setup design, Data analysis, Draft writing.

Availability of data and materials

The datasets generated (or analyzed) during the current study are available from the corresponding author on reasonable request.

Conflict of Interests

The author declare that they have no known competing financial interests or personal relationships that could have appeared to influence the work reported in this paper.

Open Access

This article is licensed under a Creative Commons Attribution 4.0 International License, which permits use, sharing, adaptation, distribution and reproduction in any medium or format, as long as you give appropriate credit to the original author(s) and the source, provide a link to the Creative Commons license, and indicate if changes were made. The images or other third party material in this article are included in the article's Creative Commons license, unless indicated otherwise in a credit line to the material. If material is not included in the article's Creative Commons license and your intended use is not permitted by statutory regulation or exceeds the permitted use, you will need to obtain permission directly from the OICC Press publisher. To view a copy of this license, visit <https://creativecommons.org/licenses/by/4.0>.

References

- [1] K. Pal, P. Singh, A. Bhaduri, and K. B. Thapa. “Current challenges and future prospects for a highly efficient ($> 20\%$) kesterite CZTS solar cell: A review.”. *Solar Energy Materials and Solar Cells*, **196**:138–156, 2019. DOI: <https://doi.org/10.1016/j.solmat.2019.03.001>.
- [2] M. Imamzai, M. Aghaeia nd Y. H. M. Thayoob, and F. Mohammadreza. “A review on comparison between traditional silicon solar cells and thin film CdTe solar cells.”. *Proceedings National Graduate Conference (NatGrad2012), Tenaga Nasional Universiti, Putrajaya Campus*, :1–5, 2012.
- [3] T. D. Leea and A. U. Ebong. “A review of thin film solar cell technologies and challenges.”. *Renewable and Sustainable Energy Reviews*, **70**:1286–1297, 2017. DOI: <https://doi.org/10.1016/j.rser.2016.12.028>.
- [4] M. A. Green, E. D. Dunlop, J. Hohl-Ebingera, M. Yoshita, N. Kopidakis, and X. Hao. “Solar cell efficiency tables (version 63)”. *Progress in Photovoltaics: Research and Applications*, **30**:3–12, 2023. DOI: <https://doi.org/10.1002/pip.3506>.
- [5] O. Rashwan, G. Sutton, and L. Ji. “Optical modeling of periodic nanostructures in ultra-thin CdTe solar cells with an electron reflector layer.”. *Superlattices Microstruct*, **149**:106757, 2021. DOI: <https://doi.org/10.1016/j.spmi.2020.106757>.
- [6] J. Ramanujam, D. M. Bishop, T. K. Todorov, O. Gunawan, J. Rath, R. Nekovei, E. Arregiani, and A. Romeo. “Flexible CIGS, CdTe and a-Si: H based thin film solar cells: A review.”. *Progress in Materials Science*, **110**:100619, 2020. DOI: <https://doi.org/10.1016/j.pmatsci.2019.100619>.
- [7] A. Luque and S. Hegedus. “Handbook of Photovoltaic Science and Engineering.”. *John Willey & Sons*, , 2011.
- [8] R. Noufi and K. Zweibel. “High-efficiency CdTe and CIGS thin-film solar cells: highlights and challenges.”. *IEEE 4th World Conference on Photovoltaic Energy Conference*, **1**:317–320, 2006. DOI: <https://doi.org/10.1109/WCPEC.2006.279455>.
- [9] H. P. Mahabaduge, W. L. Rance, J. M. Burst, M. O. Reese, D. M. Meysing, C. A. Wolden, J. Li, J. D. Beach, T. A. Gessert, W. K. Metzger, S. Garner, and T. M. Barnes. “High-efficiency, flexible CdTe solar cells on ultra-thin glass substrates.”. *Applied Physics Letters*, **106**:133501, 2015. DOI: <https://doi.org/10.1063/1.4916634>.
- [10] M. A. Islam, K. S. Rahmana, K. Sobayel, T. Enam, A. M. Ali, M. Zaman, M. Akhtaruzzaman, and N. Amin. “Fabrication of high efficiency sputtered CdS: O/CdTe thin film solar cells from window/absorber layer growth optimization in magnetron sputtering.”. *Solar Energy Materials and Solar Cells*, **172**:384–393, 2017. DOI: <https://doi.org/10.1016/j.solmat.2017.08.020>.
- [11] A. Romeo, E. Arregiani, and D. Menossi. “Low substrate temperature CdTe solar cells: A review.”. *Solar Energy*, **175**:9–15, 2018. DOI: <https://doi.org/10.1016/j.solener.2018.02.038>.
- [12] Y. G. Fedorenko, J. D. Major, A. Pressman, L. Phillips, and K. Durose. “Electronic properties of CdTe/CdS solar cells as influenced by a buffer layer.”. *MRS Advances*, **1**:937–942, 2016. DOI: <https://doi.org/10.1557/adv.2016.69>.
- [13] A. A. Al-mebir, P. Harrison, A. Kadhim, G. Zeng, and J. Wu. “Effect of in situ thermal annealing on structural, optical, and electrical properties of CdS/CdTe thin film solar cells fabricated by pulsed laser deposition.”. *Advances in Condensed Matter Physics*, , 2016. DOI: <https://doi.org/10.1155/2016/8068396>.
- [14] L. Hafaifa, M. Maache, Z. Allam, and A. Zebeir. “Simulation and performance analysis of CdTe thin film solar cell using different Cd-free zinc chalcogenide-based buffer layers.”. *Results in Optics*, **14**:100596, 2024. DOI: <https://doi.org/10.1016/j.rio.2023.100596>.
- [15] A. Hosen, B. Islam, H. Khatun, M. S. Islam, K. M. S. Rahmotullah, and S. R. Al Ahmed. “Device simulation of a highly efficient CZTS solar cell with CUS as hole transport layer.”. *IEEE International Conference on Telecommunications and Photonics (ICTP)*, , :1, 2021. DOI: <https://doi.org/10.1109/ICTP53732.2021.9744237>.
- [16] M. A. A. Noman, S. Siraj, M. J. Abden, N. Amin, and M. A. Islam. “A numerical analysis of BSF layers for ultra-thin high efficiency CdTe thin film solar cell.”. *Chalcogenide Letters*, **16**:185–193, 2019.
- [17] A. H. Mekky. “Simulation and modeling of the influence of temperature on CdS/CdTe thin film solar cell.”. *The European Physical Journal Applied Physics*, **87**:30101, 2019. DOI: <https://doi.org/10.1051/epjap/2019190037>.
- [18] O. Skhouni, A. El Manouni, B. Mari, and H. Ullah. “Numerical study of the influence of ZnTe thickness on CdS/ZnTe solar cell performance.”. *The European Physical Journal Applied Physics*, **74**:24602, 2016. DOI: <https://doi.org/10.1051/epjap/2015150365>.
- [19] X. He, Y. Song, L. Wu, C. Li, J. Zhang, and L. Feng. “Simulation of high-efficiency CdTe solar cells with Zn_{1-x}Mg_xO window layer by SCAPS software.”. *Materials Research Express*, **5**:065907, 2018. DOI: <https://doi.org/10.1088/2053-1591/aacae2>.
- [20] J. Liu, W. Chen, and X. Feng. “Numerical simulation of ultra-thin CdTe solar cells with a buffer layer of MoO_x in the backwall configuration.”. *Chinese Journal of Physics*, **56**:1826–1833, 2018. DOI: <https://doi.org/10.1016/j.cjph.2018.08.013>.

- [21] H. Fardi and F. Buny. “Characterization and modeling of CdS/CdTe heterojunction thin-film solar cell for high efficiency performance.”. *International Journal of Photoenergy*, **2013**:1–6, 2013. DOI: <https://doi.org/10.1155/2013/576952>.
- [22] N. Amina, K. Sopian, and M. Konagai. “Numerical modeling of CdS/CdTe and CdS/CdTe/ZnTe solar cells as a function of CdTe thickness.”. *Solar Energy Materials and Solar Cells*, **91**:1202–1208, 2007. DOI: <https://doi.org/10.1016/j.solmat.2007.04.006>.
- [23] G. Hashmi, M. S. Hossain, and M. H. Imtiaz. “Electrical and optical parameter-based numerical simulation of high-performance CdTe, CIGS, and CZTS solar cells.”. *Journal of Theoretical and Applied Physics*, **17**:172328, 2023. DOI: <https://doi.org/10.57647/J.JTAP.2023.1703.28>.
- [24] Atlas User’s Manual. “SILVACO Inc., Santa Clara, CA 95054, California, USA.”. , 2018.
- [25] S. M. Sze and K. K. Ng. “Physics of Semiconductor Devices.”. *John Wiley & Sons*, , 2007.
- [26] B. V. Van Zeghbroeck. “Principles of Semiconductor Devices and Heterojunctions.”. *Prentice Hall PTR*, , 2007.
- [27] R. S. Sultana, A. N. Bahar, M. Asaduzzaman, M. M. R. Bhuiyan, and K. Ahmed. “Numerical dataset for analyzing the performance of a highly efficient ultrathin film CdTe solar cell.”. *Data in Brief*, **12**:336–340, 2017. DOI: <https://doi.org/10.1016/j.dib.2017.04.015>.
- [28] R. E. Treharne, A. Seymour-Pierce, K. Durose, K. Hutchings, S. Roncallo, and D. Lane. “Optical design and fabrication of fully sputtered CdTe/CdS solar cells.”. *Journal of Physics: Conference Series*, **286**:012038, 2011. DOI: <https://doi.org/10.1742-6596/286/1/012038>.
- [29] M. Zeman, R. Swaaij, and J. Metselaar. “Optical modeling of a-Si:H solar cells with rough interfaces: Effect of back contact and interface roughness.”. *Journal of Applied Physics*, **88**:6436–6443, 2000. DOI: <https://doi.org/10.1063/1.1324690>.
- [30] M. A. Gloeckler, L. Fahrenbrucha, and J. R. Sites. “Numerical modeling of CIGS and CdTe solar cells: setting the baseline.”. *3rd World Conference on Photovoltaic Energy Conversion*, **1**:491–494, 2003. DOI: <https://doi.org/10.1109/WCPEC.2003.1305328>.
- [31] A. Cantas, F. Turkoglu, E. Meric, F. G. Akca, M. Ozdemir, E. Tarhan, L. Ozyuzer, and G. Aygun. “Importance of CdS buffer layer thickness on Cu₂ZnSnS₄-based solar cell efficiency.”. *Journal of Physics D: Applied Physics*, **51**:275501, 2018. DOI: <https://doi.org/10.1088/1361-6463/aac8d3>.
- [32] M. W. Bouabdelli, F. Rogti, M. Maache, and A. Rabehi. “Performance enhancement of CIGS thin-film solar cell.”. *Optik*, **216**:164948, 2020. DOI: <https://doi.org/10.1016/j.ijleo.2020.164948>.
- [33] M. Asaduzzaman, A. N. Bahar, M. M. R. Bhuiyan, and M. A. Habib. “Impacts of temperature on the performance of Cdte based thin-film solar cell.”. *IOP Conference Series: Materials Science and Engineering*, **225**:012274, 2017. DOI: <https://doi.org/10.1088/1757-899X/225/1/012274>.
- [34] T. N. Sultan, M. S. Farhan, and H. T. Salim AL-Rikabi. “Using cooling system for increasing the efficiency of solar cell””. *Journal of Physics: Conference Series*, **1973**:012129, 2021. DOI: <https://doi.org/10.1088/1742-6596/1973/1/012129>.
- [35] A. H. Alami. “Experimental and numerical investigation for PV cooling by forced convection.”. *Alexandria Engineering Journal*, **64**:427–440, 2023. DOI: <https://doi.org/10.1016/j.aej.2022.09.006>.
- [36] M. S. Sheik, P. Kakati, D. Dandotiya, and C. S. Ramesh. “A comprehensive review on various cooling techniques to decrease an operating temperature of solar photovoltaic panels.”. *Energy Nexus*, **8**:100161, 2022. DOI: <https://doi.org/10.1016/j.nexus.2022.100161>.